Jarzynski equality on work and free energy: Crystal indentation as a case study

The Journal of Chemical Physics

Jarzynski equality on work and free energy: Crystal indentation as a case study

Cite as: J. Chem. Phys. **156**, 114118 (2022); https://doi.org/10.1063/5.0071001
Submitted: 10 September 2021 • Accepted: 17 February 2022 • Published Online: 21 March 2022

Javier Varillas, Giovanni Ciccotti, Jorge Alcalá, et al.

The Journal of Chemical Physics ARTICLE scitation.org/journal/jcp

Jarzynski equality on work and free energy: Crystal indentation as a case study

Cite as: J. Chem. Phys. 156, 114118 (2022); doi: 10.1063/5.0071001
Submitted: 10 September 2021 • Accepted: 17 February 2022 •
Published Online: 21 March 2022

Javier Varillas,[1] Giovanni Ciccotti,[2,3,4] Jorge Alcalá,[5] and Lamberto Rondoni[6,7,a)]

AFFILIATIONS

[1] Institute of Thermomechanics, Czech Academy of Sciences, 18200 Prague, Czechia
[2] Istituto per le Applicazioni del Calcolo "Mauro Picone", IAC-CNR, Rome, Italy
[3] Dipartimento di Fisica, Università di Roma "La Sapienza", Rome, Italy
[4] School of Physics, University College Dublin (UCD), Dublin, Ireland
[5] InSup, ETSEIB, Universitat Politècnica de Catalunya, 08028 Barcelona, Spain
[6] Dipartimento di Scienze Matematiche, Politecnico di Torino, 10125 Turin, Italy
[7] INFN, Sezione di Torino, Via P. Giuria 1, 10125 Turin, Italy

[a)] **Author to whom correspondence should be addressed:** lamberto.rondoni@polito.it

ABSTRACT

Mathematical relations concerning particle systems require knowledge of the applicability conditions to become physically relevant and not merely formal. We illustrate this fact through the analysis of the Jarzynski equality (JE), whose derivation for Hamiltonian systems suggests that the equilibrium free-energy variations can be computational or experimentally determined in almost any kind of non-equilibrium processes. This apparent generality is surprising in a mechanical theory. Analytically, we show that the quantity called "work" in the Hamiltonian derivation of the JE is neither a thermodynamic quantity nor mechanical work, except in special circumstances to be singularly assessed. Through molecular dynamics simulations of elastic and plastic deformations induced via nano-indentation of crystalline surfaces that fall within the formal framework of the JE, we illustrate that the JE cannot be verified and that the results of this verification are process dependent.

I. INTRODUCTION

Statistical mechanics provides an atomistic perspective to the properties of physical systems through the correlation of mechanical and thermodynamic quantities. Certain conditions must be, however, verified in the physical system so that the formal mechanical expressions, indeed, become thermodynamically relevant.[1–6] In particular, expected values of observables dominated by the tails of their probability distributions are hard not only to estimate but also to relate to physically measurable quantities. Furthermore, emergent phenomena make certain theoretical frameworks physically insignificant, in particular, non-predictive, and require different approaches.[5] Since this depends on both the details of the process and the observable of interest, individual case-by-case analyses are required.

The Jarzynski equality (JE) has been experimentally verified mainly in small systems evolving in low dimensional spaces whose dynamics are well described by Langevin equations in Refs. 7 and 8. The original derivation of the JE concerns deterministic Hamiltonian systems,[9] and its general version given in Ref. 10 suggests that practically any kind of non-equilibrium process allows the calculation of equilibrium free-energy variations of the system under investigation. Such an apparent universality raises interesting questions, even of foundational nature.

The mechanical derivation of the JE presented in Ref. 18 takes full advantage of the canonical statistics in order to correlate the work done on a particle system (usually under non-equilibrium) as one parameter of its Hamiltonian is varied over time, while the free energy is allowed to change. This derivation is based on two main ingredients: (i) the effect of the work on the Hamiltonian, which is assumed to exclusively change one parameter λ from an initial value α to a final value ω, and (ii) the canonical ensemble at a given temperature T. Once this framework is accepted, the JE becomes fully prescribed regardless of the process that shifts λ from its initial to its final value. It, however, remains to be checked whether the conditions of the derivation are met by the systems of interest or are

violated by, e.g., emergent phenomena. Related publications, such as those discussing optimal protocols,[11–14] support the use of the JE, while others express concern.[15–17]

In a recent paper, we investigated the applicability of the JE to a variable-volume Hamiltonian system.[18] We found that the JE is not as universal as commonly believed, since it does not apply to such a paradigmatic case. In the present paper, instead, we consider a system fully described by the Jarzynski Hamiltonian. We give special attention to the presumed universality of the process that links the initial Hamiltonian with the final one.

First, we observe that the JE does not compute the free-energy difference of the bare system of interest, except in special cases (as, for instance, those described in Ref. 19). In principle, it gives an expression to compute the solvated free energy, which expresses an important property of the system of interest in interaction with its environment. Second, we perform molecular dynamics simulations to investigate a crystal nano-indentation process that fully complies with the Jarzynski formal setting. In this case, the spherical nanoscopic tip, modeled by a repulsive potential whose center moves in time, pulls downward the crystal's surface. We analyze two indentation processes that induce elastic and plastic deformations. In both cases, the Hamiltonian returns to its initial form at the end of the process. Although this fits the Jarzynski scheme in a system that is not particularly large, detailed analyses show that the JE cannot be successfully applied to either of these indentation processes. We argue that these findings are due to sampling difficulties under large values of work, as anticipated in the original JE paper.[9,20] Indeed, the exponential structure of the JE and the form of the canonical ensemble make prohibitive the use of the JE for macroscopic systems; see, e.g., Refs. 19 and 21.

Our present analysis points out that the method suggested by the JE may prevent a proper exploration of the relevant parts of the phase space even if the system is small and the process is quite mild. Moreover, it is stressed that the currently observed sampling difficulties underlie fundamental limitations when the JE is applied to analyze plastic deformation processes, which microscopically correspond to phases trapped in a limited region of the phase space. These limitations are, indeed, analogous to the strongly irreversible systems examined in Ref. 22, which fail to recover their initial state after perturbation. Since this feature cannot be solved through improved statistics, a modification of the JE appears to be at issue.

II. THE JARZYNSKI EQUALITY AND ITS MEANING

Following Ref. 10, we consider an N-particle system S interacting with an environment E made of M particles. The combined system is then denoted as S + E, which is made of $N + M$ particles. Let $\Gamma = (x, y)$ represent a mechanical state of S + E in the phase space $\mathcal{M}$, with $x = (q_S, p_S)$ with the coordinate vector $q_S = (q_1, \ldots, q_N)$ and momenta $p_S = (p_1, \ldots, p_N)$ of S, and $y = (q_E, p_E)$ representing E, with $q_E = (q_{N+1}, \ldots, q_{N+M})$ and $p_E = (p_{N+1}, \ldots, p_{N+M})$.

Suppose an external agent perturbs S in such a way that only the energy H_S of S is affected, where the energy H_E of E and the energy of the interaction between S and E, h_{int}, are not directly affected. While this is not a general condition in Ref. 6, it is our purpose to focus on systems for which this assumption holds. Moreover, let the perturbation be described by a time dependent parameter, $\lambda \in \mathbb{R}$, that varies according to a specified rule $\lambda(t)$, with $t \in [0, \tau]$, $\lambda(0) = \alpha$, and $\lambda(\tau) = \omega$. Under these assumptions, the dynamics of the particles of the combined system S + E may be described by the following Hamiltonian:

$$\mathcal{H}(\Gamma; \lambda) = H_S(x; \lambda) + H_E(y) + h_{int}(x, y). \tag{1}$$

For the sake of simplicity, and as commonly done, let us assume that the external agent acts on such a mechanical system by exerting on the particles of S forces that derive from an external potential Φ,

$$F_i = -\frac{\partial \Phi}{\partial q_i}, \quad i = 1, \ldots, N. \tag{2}$$

The Hamiltonian system S + E is initially in thermodynamic equilibrium with a heat bath B at temperature T. Hence, its initial phases are distributed according to the canonical ensemble with parameter $\lambda(0) = \alpha$,

$$f_\alpha(\Gamma) = \frac{e^{-\beta \mathcal{H}(\Gamma; \alpha)}}{\mathcal{Q}_{S+E}(\alpha)},$$

with

$$\mathcal{Q}_{S+E}(\lambda) = \int e^{-\beta \mathcal{H}(\Gamma; \lambda)} d\Gamma, \tag{3}$$

where $\beta = 1/k_B T$ and $\mathcal{Q}_{S+E}(\lambda)$ is the canonical partition function of a system at temperature T, with Hamiltonian $\mathcal{H}(\Gamma; \lambda)$. At time $t = 0$, when the phase of S + E is $\Gamma_0 = (x_0, y_0)$, the energy is $\mathcal{H}(\Gamma_0; \alpha)$ and S + E is separated from B. Then, λ is allowed to change for $t \in (0, \tau)$.

Let $S^t_\lambda : \mathcal{M} \to \mathcal{M}$ denote the evolution operator for time t for the phases in $\mathcal{M}$, meaning that an initial phase $\Gamma \in \mathcal{M}$ turns into $S^t_\lambda \Gamma \in \mathcal{M}$ at time t. The process stops at time $t = \tau$, when $\lambda(\tau) = \omega$, and the Hamiltonian of S + E is expressed by $\mathcal{H}(\Gamma; \omega)$. On the other hand, the energy of the realization of the process with initial condition Γ_0 is given by $\mathcal{H} = \mathcal{H}(\Gamma_\tau; \omega)$, where $\Gamma_\tau = (x_\tau, y_\tau) = S^\tau_\lambda \Gamma_0$ denotes the final phase. Although obvious, it is important to remark the difference between the energy of the system at the end of the process, which is $\mathcal{H}(\Gamma_\tau; \omega)$, and the Hamiltonian with parameter $\lambda = \omega$ at a generic phase point Γ, which is $\mathcal{H}(\Gamma; \omega)$. The former, indeed, is not the Hamiltonian, but the composition of the Hamiltonian with the time evolution up to time τ, S^τ_λ.

Let $q_i(t; \Gamma)$ be the coordinates of particle i at time t, along the phase space trajectory starting at Γ, and $p_i(t; \Gamma)$ be the corresponding momenta. Then, in the time interval $[0, \tau]$, the external agent determining the variation of λ performs a mechanical work on S, expressed by

$$W\left[S^t_\lambda \Gamma; 0 \le t \le \tau\right] = \int_0^\tau ds \sum_{i=1}^N \dot{q}_i(s; \Gamma) \cdot F_i(S^s_\lambda \Gamma), \tag{4}$$

which, in this deterministic framework, depends only on the initial condition Γ and on the chosen function $\lambda = \lambda(t)$. For such a process, W can take positive, null, and also negative values depending on Γ. In the Jarzynski theory, the term "work" is used, instead, for a different quantity, which we denote as W_J and is defined by

$$W_J\left[S^t_\lambda \Gamma; 0 \le t \le \tau\right] = \int_0^\tau ds\, \dot{\lambda}(s) \frac{\partial H_S}{\partial \lambda}(x_s; \lambda(s)). \tag{5}$$

Obviously, this corresponds to mechanical work when λ represents a position in space and the derivative of H_S with respect to λ is a force.[23] Because the following equation holds:

$$\frac{\partial H_S}{\partial t} = \dot{\lambda}\frac{\partial H_S}{\partial \lambda} = \dot{\lambda}\frac{\partial \mathcal{H}}{\partial \lambda} = \frac{\partial \mathcal{H}}{\partial t} = \frac{\mathrm{d}\mathcal{H}}{\mathrm{d}t}, \tag{6}$$

one obtains

$$W_J\left[S_\lambda^t\Gamma; 0 \le t \le \tau\right] = \mathcal{H}(S_\lambda^\tau\Gamma;\omega) - \mathcal{H}(\Gamma;\alpha). \tag{7}$$

Equation (7), exponentiated and averaged over the canonical ensemble at temperature T and parameter $\lambda = \alpha$, straightforwardly leads to

$$\left\langle e^{-\beta W_J}\right\rangle_\alpha = \frac{1}{\mathcal{Q}_{S+E}(\alpha)}\int e^{-\beta W_J(\Gamma)}e^{-\beta\mathcal{H}(\Gamma;\alpha)}\,\mathrm{d}\Gamma = \frac{\mathcal{Q}_{S+E}(\omega)}{\mathcal{Q}_{S+E}(\alpha)} = e^{-\beta[F_{S+E}(\omega)-F_{S+E}(\alpha)]}, \tag{8}$$

where $\Delta F_{S+E} = [F_{S+E}(\omega) - F_{S+E}(\alpha)]$ is the difference of the free energies of S + E in the canonical equilibrium at temperature T and parameters ω and α, respectively. Given the exponential form of the quantity to be averaged in Eq. (8), it is readily seen that large negative values of W_J give important contributions, even if they are very unlikely in the canonical ensemble f_α.

As far as we understand, the desired result in Refs. 9 and 10 is not ΔF_{S+E}, but the free-energy difference for system S alone, defined by

$$\Delta F_S = [F_S(\omega) - F_S(\alpha)], \quad F_S(\lambda) = -\beta^{-1}\ln\mathcal{Q}_S(\lambda), \quad \mathcal{Q}_S(\lambda) = \int \mathrm{d}x\, e^{-\beta H_S(x;\lambda)}. \tag{9}$$

The quantity F_S is the "*intrinsic*" free energy of S; it is particularly interesting when h_{int} vanishes. Jarzynski, indeed, originally assumed that h_{int} is negligible compared to H_S and H_E.[9] In this case, and under the assumption that S remains isolated, consequently,

$$F_{S+E}(\lambda) = F_S(\lambda) + F_E, \quad \lambda = \alpha, \omega$$

and

$$\Delta F_{S+E} = \Delta F_S, \tag{10}$$

since in the difference, the free energy of E cancels out. However, this framework is not satisfactory for the kinds of experiments that the JE is mainly supposed to describe. When h_{int} is not negligible, it becomes appropriate, as argued also by Jarzynski,[24] to consider a quantity that accounts for such an interaction, and this is called solvated free energy. The derivation of the JE then proceeds introducing the following Hamiltonian:

$$H_S^*(x;\lambda) = H_S(x;\lambda) - \frac{1}{\beta}\ln\frac{\int \mathrm{d}y e^{-\beta[H_E(y)+h_{\mathrm{int}}(x,y)]}}{\int \mathrm{d}y e^{-\beta H_E(y)}} \tag{11}$$

which was proposed by Kirkwood[25] to treat subsystems of macroscopic dense fluids in thermodynamic equilibrium.[26] This is the energy of S, H_S, referred to the interaction energy averaged over the variables of E, which essentially amounts to a potential of mean force. Its meaning can be understood in terms of the marginal probability of the particles of S in E,

$$p_S(x;\lambda) = \int \mathrm{d}y\, f_\lambda(x,y) = \frac{e^{-\beta H_S(x;\lambda)}}{\mathcal{Q}_{S+E}(\lambda)}\int \mathrm{d}y\, e^{-\beta\{H_E(y)+h_{\mathrm{int}}(x,y)\}}, \tag{12}$$

whose associated Landau free energy takes the form

$$-\frac{1}{\beta}\log p_S(x;\lambda) = -\frac{1}{\beta}\log\left[\frac{e^{-\beta H_S(x;\lambda)}}{\mathcal{Q}_{S+E}(\lambda)}\int \mathrm{d}y\, e^{-\beta\{H_E(y)+h_{\mathrm{int}}(x,y)\}}\right] = F_{S+E}(x;\lambda). \tag{13}$$

This shows that H_S^* is the effective Hamiltonian of S in S + E. Indeed, we can write

$$H_S^*(x;\lambda) = F_{S+E}(x;\lambda) - \frac{1}{\beta}\log\frac{\mathcal{Q}_{S+E}(\lambda)}{\mathcal{Q}_E} = F_{S+E}(x;\lambda) + \text{constant}, \tag{14}$$

where the constant is absorbed by the normalization condition. The associated canonical partition function takes the form

$$\mathcal{Q}_S^*(\lambda) = \int \mathrm{d}x\, e^{-\beta H_S^*(x;\lambda)}\mathrm{d}x = \int \mathrm{d}x\, e^{-\beta H_S(x;\lambda)}\frac{\int \mathrm{d}y\, e^{-\beta[H_E(y)+h_{\mathrm{int}}(x,y)]}}{\int \mathrm{d}y\, e^{-\beta H_E(y)}} = \frac{\int e^{-\beta\mathcal{H}(\Gamma;\lambda)}\,\mathrm{d}\Gamma}{\int e^{-\beta H_E(y)}\,\mathrm{d}y} = \frac{\mathcal{Q}_{S+E}(\lambda)}{\mathcal{Q}_E}. \tag{15}$$

The logarithm of $\mathcal{Q}_S^*(\lambda)$ multiplied by $-\beta$ yields

$$F_S^*(\lambda) = F_{S+E}(\lambda) - F_E, \quad \textit{i.e.} \quad F_{S+E}(\lambda) = F_S^*(\lambda) + F_E, \tag{16}$$

where $F_S^*(\lambda) = -\beta^{-1}\ln\mathcal{Q}_S^*(\lambda)$ is the "*solvated*" free energy that can be interpreted as the free energy of a hypothetical system S* with Hamiltonian H_S^* or of "*S in E*," and

$$F_E = -\beta\ln\int e^{-\beta H_E(y)}\,\mathrm{d}y \tag{17}$$

is the free energy of E alone in thermodynamic equilibrium at temperature T. Now, the free energy of S + E is given by the sum of the two contributions, taken separately, as if S* and E were not interacting or the interaction was negligible. Consequently,

$$[F_{S+E}(\omega) - F_{S+E}(\alpha)] = \left[F_S^*(\omega) - F_S^*(\alpha)\right] \equiv \Delta F_{\alpha\to\omega}^*, \tag{18}$$

because in this investigation, F_E does not depend on λ. Therefore, denoting by $\langle\cdot\rangle_\alpha$, a canonical average with respect to the *initial* ensemble f_α, one can finally write

$$\left\langle e^{-\beta W_J}\right\rangle_\alpha = e^{-\beta\Delta F_{\alpha\to\omega}^*}, \tag{19}$$

which is the JE. Could one assume

$$\Delta F_{\alpha\to\omega}^* = F_S(\omega) - F_S(\alpha), \tag{20}$$

with F_S standing for the intrinsic free energy of S defined in Eq. (9), the JE would then provide the difference of such physically relevant free-energy variation from the statistics of W_J. However, the previous derivation reveals that F_S^* and F_S are far from equivalent. In fact, when $\lambda = \alpha$, F_S^* depends on the environment in a different fashion than when $\lambda = \omega$. On the contrary, F_S should not depend on E whatsoever. Apart from such an unneglectable fact, the derivation of the JE is formally quite general and applicable to any particle system, under any kind of perturbation of an initial equilibrium state at a given temperature T. Indeed, no restrictions are imposed on the time dependence of λ. Summing up, we note that the Jarzynski approach does not separate the degrees of freedom of S and E unless the interaction term $h_{\rm int}$ is negligible or absent. Then, different environments lead to different estimates of the solvated free energy F_S^*, which, in general, differ from the intrinsic free energy F_S. In the early Hamiltonian derivations, the focus was on F_S. Later, the solvated free energy has become the focus of the Hamiltonian derivations, which is relevant under strong coupling between S and E.

A related observation concerns W_J. In general, this quantity is directly related neither to mechanical nor to thermodynamic work; cf. Ref. 18 and references therein. It is not related to mechanical work since, without further specification, the derivative of H_S with respect to λ is not a force, and $\mathrm{d}\lambda = \dot{\lambda}\mathrm{d}t$ is not an associated elementary displacement. In particular, the Hamiltonian may depend on a time dependent parameter in many different fashions that do not correspond to displacements of the external driving mechanism. Moreover, averaging W_J with respect to the initial ensemble, one obtains

$$\begin{aligned}\langle W_J\rangle_\alpha &= \int \mathcal{H}(S_\lambda^\tau\Gamma;\omega)\,\frac{e^{-\beta\mathcal{H}(\Gamma;\alpha)}}{\mathcal{Q}_{S+E}(\alpha)}\mathrm{d}\Gamma \\ &\quad - \int \mathcal{H}(\Gamma;\alpha)\,\frac{e^{-\beta\mathcal{H}(\Gamma;\alpha)}}{\mathcal{Q}_{S+E}(\alpha)}\mathrm{d}\Gamma \\ &= U^*(\tau,\omega) - U(\alpha). \end{aligned} \tag{21}$$

Here, the second integral, $U(\alpha)$, is the initial internal energy of S + E, because of the average of the initial Hamiltonian with respect to the initial canonical ensemble. On the other hand, the first integral, $U^*(\tau,\omega)$, is the average of the Hamiltonian of S + E with parameter ω computed in a τ-dependent position,

$$u_{\omega,\tau}(\Gamma) = \left[\mathcal{H}(\cdot;\omega)\circ S_\lambda^\tau\right](\Gamma) = \mathcal{H}(S_\lambda^\tau\Gamma;\omega),$$

so that it is not the Hamiltonian with parameter ω, but a function of function, with $\mathcal{H}(\cdot;\omega)$ as an external function, averaged with respect to the initial ensemble f_α.[27] Only the average of the exponential of W_J, not of W_J itself, appears to be directly associated with a known physical quantity. Although computable in numerical simulations, W_J and $\langle W_J\rangle_\alpha$, are hardly relevant in experiments except, in particular, situations to be identified case by case.[18]

The numerical simulations discussed in Secs. III–V correspond to a case intentionally chosen so that W_J results in a measurable mechanical work. Then, we investigate the presumed process independence of the JE, remaining within the bounds of the Jarzynski theory. We show that the process affects the results, as natural in physics. In particular, we investigate a Hamiltonian system describing indentation on a small crystal made of $O(10^4)$ particles. We realize closed work loops, i.e., processes for which $\lambda(0) = \lambda(\tau)$, where the right-hand side of Eq. (19) should take unity. Thus, we consider the case involving elastic deformations of the crystal, which is reversible and should lead to no surprise. In addition, we study the irreversible case of plastic deformations, in which the impossibility for the system to close the loop shows an emergent property of (even relatively small) Hamiltonian systems.[28] In both the cases, we find that it is impossible to verify the JE, although we remain within the Jarzynski framework. As for the claims that the JE should be invoked in the case of small systems only, we note that the number of particles in our system is not larger than those of proteins and DNA used in the experiments assessing the JE.[29]

III. CRYSTAL INDENTATION

A. The simulation

In the following, we systematically investigate the properties of a small solid indented by a spherical nanoscopic tip. The solid of interest is a (001)-oriented Ta crystal of size $10.8 \times 10.8 \times 6$ nm^3 made of $N_{\rm tot} = 40,293$ particles, whose coordinates are denoted by

$$q_i = (x_i, y_i, z_i) \qquad i = 1, \ldots, N_{\rm tot}. \tag{22}$$

The particles in the top layer of the solid are free to move, whereas those in the bottom layer are fixed and constitute a rigid flat surface that prevents the downward displacement of the system during indentation. Periodic boundary conditions are applied on the lateral sides of the crystal; see Fig. 1(a). In the Jarzynski theory, in contact with the rigid flat can be taken to represent an external field, which does not contribute to the number $N_{\rm tot}$. Because only the top layers of the crystal are affected by the action of the indenter, we may indifferently consider the solid as a whole or just the top N particles as system S without any expected change in the numerical results. The remaining $M = N_{\rm tot} - N$ particles, which are not brought into contact with the indenter, will then be considered as the environment E. One way or the other, the dynamics is determined by a Hamiltonian of the likes of Eq. (1), which turns $\mathcal{H} = H_S$ in the first case. Note, however, that the JE is, in principle, an immediate consequence of the Hamiltonian dynamics and of the canonical statistics for $N = N_{\rm tot}$, while further assumptions are required for $N < N_{\rm tot}$. This ambiguity is consistent with the fact in that the JE only computes the free-energy variations of the whole S + E.

Our investigation comprises an extensive number of all-atom molecular dynamics (MD) simulations performed with the LAMMPS code.[30] The indenter is modeled by a time-dependent spherically symmetric, repulsive external potential of finite range, with $R = 3$ nm and center C of coordinates $q_c(t) = (x_c, y_c, z_c(t))$, defined by

$$\begin{aligned}\Phi(q_1,\ldots,q_{N+M},q_c(t)) &= \sum_{i=1}^{N+M}\varphi(q_i,q_c(t)); \\ \varphi(q_i,q_c(t)) &= \begin{cases} -k\delta_i(t)^3/3, & \delta_i \le 0, \\ 0, & \delta_i > 0, \end{cases}\end{aligned} \tag{23}$$

where k is the indenter stiffness and

$$\delta_i(t) = \sqrt{(x_i - x_c)^2 + (y_i - y_c)^2 + (z_i - z_c(t))^2} - R \tag{24}$$

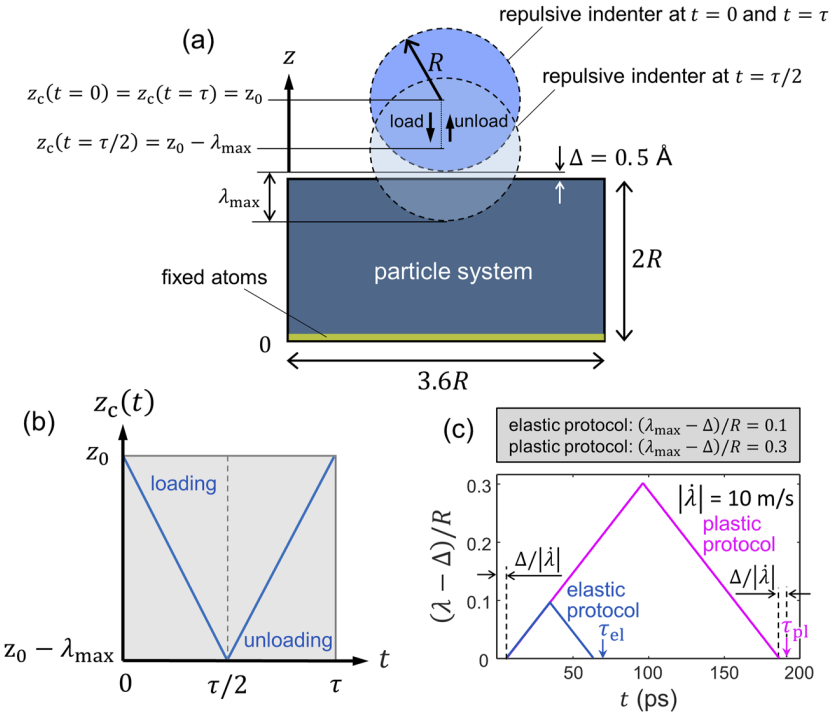

FIG. 1. Simulation setup. (a) Schematic representation of the indentation process. The computational domain contains the particle system of size $3.6R \times 3.6R \times 2R$ and the repulsive spherical indenter of radius R modeled by Eq. (23). Periodic boundaries are applied to the lateral sides of the cells. The indented top surface is free while the atomic positions in the bottom atomic layer are fixed to prevent the downward displacement of the particle system during indentation. The vertical coordinate of the indenter center, z_c, is plotted in (b) as a function of the process time τ. (c) Evolution of the quantity $(\lambda - \Delta)/R$ as a function of t in the elastic and plastic cases with $|\dot{\lambda}| = 10$ m/s whose process times are $\tau_{el} = 70$ ps and $\tau_{pl} = 190$ ps, respectively.

is positive if particle i is outside the range of action of Φ and negative if it is inside. The indenter acts on the particles of the solid that lie within a distance R from the center C, and there is no recoil in the system because the atoms of the bottom layer are fixed. This places our system in the laboratory frame. Here, k is set to 100 eV/Å^3 ($\approx 1.6 \times 10^{-10}$ erg/Å^3). This computational approach has been largely employed in MD investigations of nano-indentation on metal surfaces (cf. Refs. 31–34). Figure 1(a) depicts the computational domain of the indentation simulations, which contains the particle system and the repulsive indenter.

In the present simulations, we take an initial state in which particles lie at their crystal lattice positions, and velocities are taken from a normal distribution with 0 mean and a standard deviation chosen to produce a temperature close to $T = 300$ K. Then, in order to generate the equilibrium canonical distribution in the phase space of the system [Eq. (3)], we carry out a preliminary 20-ps thermalization run during which the particles follow the NVT ensemble where the system's volume remains fixed and the Nosé–Hoover thermostat controls the system's temperature. This allows us to produce a large set of n initial conditions that sample the canonical distribution f_α at $T = 300$ K, from which each load–unload indentation process is carried out.

A closed indentation load loop is realized by letting z_c move vertically with constant downward and upward speeds, $\dot{\lambda}$. The vertical coordinate of the indenter center, $z_c(t)$, then follows

$$z_c(t) = z_0 - \lambda(t), \quad \text{with} \quad |\dot{\lambda}| = \text{const},$$
$$\lambda(t) = \begin{cases} |\dot{\lambda}|t, & t \in [0, \tau/2), \\ |\dot{\lambda}|(\tau - t), & t \in [\tau/2, \tau], \end{cases} \tag{25}$$

where λ reaches its maximum, λ_{max}, at time $t = \tau/2$, with $z_c(\tau/2) = z_0 - \lambda_{max}$ and $\tau = 2\lambda_{max}/|\dot{\lambda}|$; see Fig. 1(b). Thus, we have $\lambda(\alpha) = \lambda(\omega)$. During the indentation run, the particle dynamics is given by Hamilton's equations of motion under the following time-dependent Hamiltonian:

$$\mathcal{H}(\Gamma) = \sum_{i=1}^{N+M} \frac{1}{2} m v_i^2 + \Omega(q_1, \ldots, q_{N+M}) + \Phi(q_1, \ldots, q_{N+M}, q_c(t)), \tag{26}$$

where m is the mass of each Ta atom and $v_i = \sqrt{v_{ix}^2 + v_{iy}^2 + v_{iz}^2}$ is the speed of particle i. The constituting Ta particles of the crystal interact with each other via the embedded-atom method (EAM) potential built by Ravelo *et al.*[35] This model is based on concepts from density functional theory that stipulate that the (potential) energy of atom i, Ω_i, is a function of the spatially dependent electron density. The potential energy of the system, Ω, is then prescribed by the following EAM functions:

$$\Omega = \sum_{i=1}^{N+M} \Omega_i, \quad \Omega_i = E^*(\bar{\rho}_i) + \frac{1}{2} \sum_{i \neq j=1}^{N+M} \phi(r_{ij}), \quad \bar{\rho}_i = \sum_{i \neq j=1}^{N+M} w(r_{ij}), \tag{27}$$

where r_{ij} is the distance between atoms i and j, ϕ is a pairwise, spherically symmetric interaction potential, $\bar{\rho}_i$ is the electron density at site i, which is taken proportional to the atomic density surrounding the site and given by a sum of spherically symmetric weights w evaluated

at the pairs distances, $E^*(\bar{\rho}_i)$ is the embedding energy, a nonlinear function of the electron density, and ϕ is expressed by

$$\phi(r) = \begin{cases} -U_0\left(1 + r^* + \beta_3 r^{*3} + \beta_4 r^{*4}\right)e^{-r^*}, & 0 \le r \le r_s, \\ U_0(r_c - r)^s \sum_{i=1}^{4} a_i (r_c - r)^{i-1}, & r_s < r \le r_c, \\ 0, & r > r_c, \end{cases} \quad (28)$$

where $r^* = \alpha_p(r/r_1 - 1)$ and $\alpha_p, r_1, r_c, r_s, s, U_0, \beta_3$, and β_4 are the fitting parameters adjusted to Ta atoms.[35]

Note that no thermostat is coupled to S + E during the indentation process, as required by Jarzynski's theory. The integration time step is set to 2 fs in all the MD simulations.

B. Computation of work fluctuations during indentation

The simulated particles may be indifferently taken to constitute S + E, or just S, as the short range potential Φ only affects the first few atomic layers of the solid, and the particles close to the bottom flat do not approach those at the top layers in any physically imaginable time. In particular, taking E as the bottom half of the solid, so that $N = M$, is more than sufficient to make sure that the indenter does not contact the environment; see Fig. 1.

The repulsive force exerted on particle i, $F_i = -(\partial\Phi/\partial q_i)$, where Φ is the only time-dependent term in the Hamiltonian, is given by

$$(F_{ix}, F_{iy}, F_{iz}) = \begin{cases} k\delta_i^2 (x_i - x_c, y_i - y_c, z_i - z_c)/(\delta_i + R), & \delta_i \le 0, \\ 0, & \delta_i > 0. \end{cases} \quad (29)$$

The elementary mechanical work done by the indenter on S is expressed in terms of the elementary particle displacements, $\mathrm{d}q_i = (\mathrm{d}x_i, \mathrm{d}y_i, \mathrm{d}z_i)$, through

$$\begin{aligned} \mathrm{d}W_{I\to S} &= \sum_{i=1}^{N} F_i \cdot \mathrm{d}q_i \\ &= \sum_{i=1}^{N} \frac{k\,\delta_i^2\,\eta(\delta_i)}{\delta_i + R}\left[(x_i - x_c)\mathrm{d}x_i + (y_i - y_c)\mathrm{d}y_i \right. \\ &\quad \left. + (z_i - z_c)\mathrm{d}z_i\right], \end{aligned} \quad (30)$$

where η is the step function: $\eta(\delta_i) = 1$ for $\delta_i \le 0$ and $\eta(\delta_i) = 0$ for $\delta_i > 0$. The elementary work done on the indenter by S, which involves instead the elementary displacements of the indenter, $\mathrm{d}q_c = (0, 0, \mathrm{d}z_c)$, and the opposite forces, $-F_i$, is given by

$$\begin{aligned} \mathrm{d}W_{S\to I} &= \sum_{i=1}^{N} (-F_{iz})\,\mathrm{d}z_c \\ &= -\sum_{i=1}^{N} \frac{k\,\delta_i^2\,\eta(\delta_i)}{\delta_i + R}\,(z_i - z_c)\,\mathrm{d}z_c \neq -\mathrm{d}W_{I\to S}, \end{aligned} \quad (31)$$

moreover, $\mathrm{d}z_c = -\mathrm{d}\lambda = -\dot{\lambda}\,\mathrm{d}t$; hence, (32)

$$\begin{aligned} \mathrm{d}W_{S\to I} &= -\sum_{i=1}^{N} \frac{k\,\delta_i^2\,\eta(\delta_i)}{\delta_i + R}\,(z_i - z_c)\,(-\dot{\lambda})\,\mathrm{d}t \\ &= \sum_{i=1}^{N} F_{iz}\,\dot{\lambda}\,\mathrm{d}t \end{aligned} \quad (33)$$

where the minus sign in the force of particle i on the indenter is derived from the action–reaction principle. Note that the mechanical works $\mathrm{d}W_{I\to S}$ and $\mathrm{d}W_{S\to I}$ differ not only in the sign, but substantially. Therefore, an external operator cannot deduce the work done on the system $W_{I\to S}$ from (external) measurements of $W_{S\to I}$. Under these conditions, the elementary Jarzynski work [from Eq. (5)], in turn, takes the form

$$\mathrm{d}W_{\mathrm{J}} = \dot{\lambda}\frac{\partial H_{\mathrm{S}}}{\partial\lambda}\mathrm{d}t = \dot{\lambda}\frac{\partial\Phi}{\partial\lambda}\mathrm{d}t = \sum_{i=1}^{N}(-F_{iz})\,\dot{\lambda}\,\mathrm{d}t = -\mathrm{d}W_{S\to I}. \quad (34)$$

W_{J} equals, in this case, the opposite of the work done by the system on the indenter.

IV. RESULTS

In the indentation protocols, we conveniently take z_0 separated by a vertical distance $R + \Delta$ from the crystal's surface so that the constituting particles are guaranteed to lie outside the range of Φ at $t = 0$ and $t = \tau$; see Fig. 1(a). This effectively allows the particles to arrange initially into an unperturbed Ta bcc crystal configuration during the canonical thermalization run. The *indenter* then exerts a localized repulsive force on the particles when they enter the indenter's range of action, thus mimicking the mechanical conditions of ultra-low load indentation experiments using an infinitely rigid indenter tip. For fixed $\dot{\lambda}$ and τ, the imposed $\lambda_{\max}$ value that characterizes the indentation process prescribes the minimum value of z_c, which is $[z_0 - \lambda(\tau/2)]$; see Fig. 1. The load $P = -\sum_{i=1}^{N} F_{iz}$ applied by the indenter is defined as the sum of the vertical, repulsive force contributions coming from the particles that satisfy $\delta_i \le 0$. Finally, the works defined by Eqs. (30), (33) and (34) are systematically computed with a fixed range of values of λ, $|\Delta\lambda| = 5$ pm (=0.05 Å), where $\mathrm{d}t = |\Delta\lambda|/|\dot{\lambda}|$.

A. The elastic case

We perform an extensive number of load/unload indentations with fixed $\lambda_{\max} = 0.1R + \Delta = 3.5$ Å, which characterizes the herein called elastic process. Our analysis includes a wide range of indentation velocities, $|\dot{\lambda}|$, from 1 to 100 m/s, which are, nevertheless, microscopically quite slow processes (corresponding to 10^{-5}–10^{-3} Å/fs in microscopic units). Thus, the imposed indenter velocities are not exceedingly violent for a particle system to endure, and the process avoids the emergence of evident irreversibility.

The computation of single-realization runs of the elastic process indicates that perturbations of the crystal with $|\dot{\lambda}| < 50$ m/s lead to elastic contacts of the indenter with the particle system. Under these conditions, the unloading stage approximately traces back the mechanical path followed during loading, thus manifesting *reversibility* in the protocols. This is shown in Figs. 2(a) and 2(b), where the applied indentation load, P, is plotted against λ and the normalized time t/τ, respectively. The elastic load–unload curves adhere to the continuum Hertzian solution that follows $P \sim (\lambda - \Delta)^{3/2}$.[36]

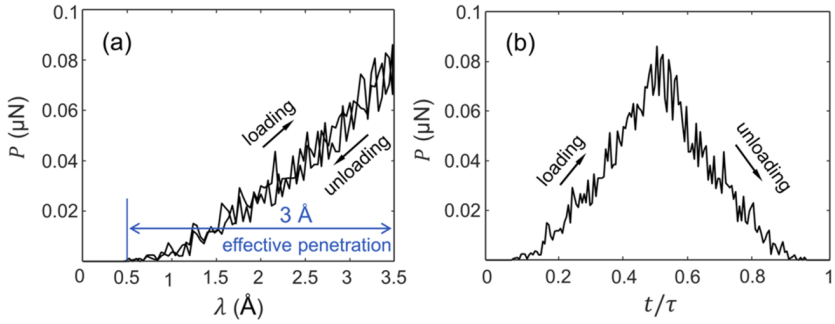

FIG. 2. Single realization of the elastic process at $|\dot{\lambda}| = 10$ m/s ($\tau = 70$ ps), where $\lambda_{max} = 3.5$ Å. (a) and (b) $P - \lambda$ and $P - t/\tau$ curves, respectively. In panel (a), the reversibility of the protocol is revealed by matching the load and unload paths. "Loading" and "unloading" mark the P direction during the loading, $t \in [0,\tau/2)$, and unloading, $t \in [\tau/2, \tau]$, of the indenter.

The reversibility of the elastic perturbation also becomes evident in the work vs λ plots in Fig. 3(c). In the same vein, Fig. 3(d) shows the symmetry of both $W_{S\to I}$ and W_J as a function of t/τ. Note that the sharp points at $t = \tau/2$ in Figs. 2(b) and 3(d) are due to the fact that the motion of the indenter is inverted, while the exerted forces from the indenter at $t = (\tau/2)^-$ and $t = (\tau/2)^+$ remain the same. Thus, along the time interval $[0, \tau]$, the absolute values of W_J and $W_{S\to I}$ gradually increase from 0 to the maximum value at time $\tau/2$ and then decrease during unloading, matching the loading work path. For comparison, the much more noisy time evolution of the work done on S, $W_{I\to S}$, is drawn in Fig. 3(a). The inset of shows the absolute values of $W_{I\to S}$, which are continuous increasing functions of time. In this regard, the net values that $W_{I\to S}$ takes as a function of time largely diverge from those of W_J and $W_{S\to I}$, where $W_{I\to S}(t = \tau) \gg 0$; compare Fig. 3(a) with Fig. 3(b).

The probability density function (PDF) describing the resulting W_J-value statistics from n realizations of a given elastic indentation can be approximated by the general form of the normal Gaussian distribution,

$$g(W_J, \mu, \sigma) = \frac{1}{\sigma\sqrt{2\pi}} \exp\left[\frac{-(W_J - \mu)^2}{2\sigma^2}\right], \tag{35}$$

where μ is the average and σ^2 is the variance of the W_J data. In all instances, W_J stands for $W_J(\tau)$. Figure 4 shows the resulting PDF of the elastic case, obtained from 1000 realizations. The results of different values for the imposed indenter velocity, $|\dot{\lambda}|$, are considered next; see Fig. 4(a). With decreasing values of $|\dot{\lambda}|$, one gradually obtains indentations in which the noise associated with P during mechanical loading and unloading is substantially reduced. Accordingly, the PDFs of the W_J data shift toward $\mu \to 0$ with decreasing $|\dot{\lambda}|$; see Fig. 4(a). In the event that this yielded quasi-static indentation transformations, with increasingly narrower W_J distributions ($\sigma \to 0$), one would not need much statistics in the $|\dot{\lambda}| \to 0$ limit. For the $|\dot{\lambda}| = 10$ m/s case, Fig. 4(b) shows that increasing the sample size ($n > 500$) does not lead to substantial changes in the resulting W_J distribution.

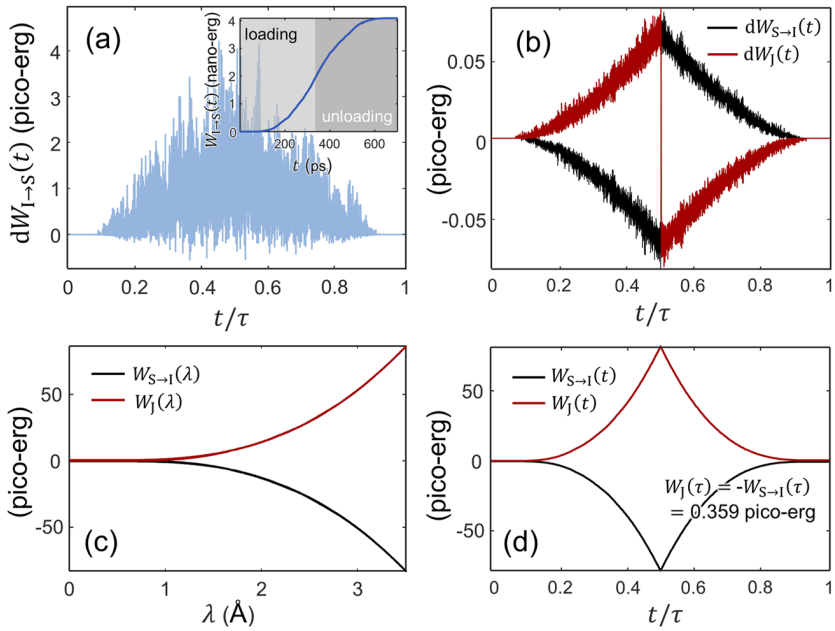

FIG. 3. Evolution of the three works defined in Eqs. (30)–(34). The plots refer to a single realization of the elastic protocol at $|\dot{\lambda}| = 1$ m/s, with $\tau = 700$ ps. dW stands for the work done in an infinitesimal time $dt = 5$ ps. (a) $dW_{I\to S}$ vs t/τ, with the time average of about $9k_BT$ (at $T = 300$ K). The time evolution of $W_{I\to S}$ is given in the inset to (a). (b) dW_J and $dW_{S\to I}$ vs t/τ. (c) and (d) Evolution of W_J and $W_{S\to I}$ as functions of λ and t/τ, respectively. In the inset to (a), in (c), and in (d), the works are the cumulative sum of the sequence of corresponding elementary works.

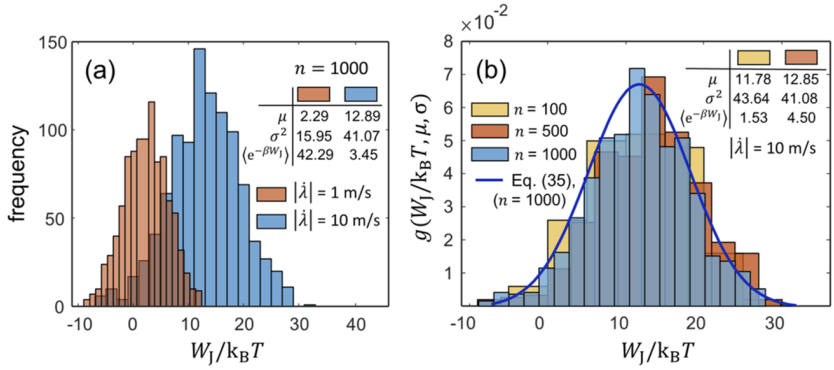

FIG. 4. W_J statistics of the elastic case. (a) W_J histograms under $|\dot{\lambda}| = 1$ and 10 m/s. (b) The resulting PDFs from 100, 500, and 1000 realizations at $|\dot{\lambda}| = 10$ m/s, which shows the saturation of moments with the ensemble size n.

Using the W_J data from the indentation realizations, the computed average of the exponential, $\langle e^{-\beta W_J} \rangle$ (where in present simulations, $\beta = 24.143$ pico-erg^{-1}), results in 3.4 and 42.3 for $|\dot{\lambda}| = 10$ and 1 m/s, respectively; see Fig. 4(a). Using the same data, the free-energy difference $\Delta F^*_{\alpha\to\omega}$ obtained from the JE [Eq. (19)] stabilizes (as visible for $n > 500$) at ≈ -0.4 pico-erg for $|\dot{\lambda}| = 1$ m/s and at ≈ -0.12 pico-erg for $|\dot{\lambda}| = 10$ m/s; cf. Fig. 9 below. We also observe stabilization of the W_J data moments with increasing sample size; cf. Fig. 4(b). In light of these results, we cannot expect the theoretical result, $\Delta F^*_{\alpha\to\omega} = 0$, to be obtained in any physically sensible observation scale.

Different indentation responses are obtained for indenter speeds $|\dot{\lambda}|$ larger than 50 m/s. These indentations are characterized by marked undulations in the $P - \lambda$ curves; see the plots in Figs. 5(a) and 5(b) obtained with $|\dot{\lambda}| = 100$ m/s. This suggests that we have a solid-to-solid impact rather than a continuous elastic contact. The results from the single-realization runs shown in Fig. 5(a) reveal that although the unloading force also vanishes at the end of the loading loop, the load and unload $P - \lambda$ paths are not identical. Thus, although the elasticity threshold of the solid is not exceeded, some kind of irreversibility progressively builds up as the speed of the indenter is increased.

Finally, we note in Fig. 5(c) that the W_J distribution obtained from 2000 realizations yields a much larger absolute value of the average of W_J [$\mu = 31.3226$ pico-erg, $\approx$756 in dimensionless $W_J/(k_B T)$ units at $T = 300$ K] as compared to that obtained in the indentations with smaller $|\dot{\lambda}|$ (Fig. 4). Then, under the fast elastic protocols, Eq. (19) gives an even worse estimate of the free-energy variation than that obtained in slow elastic processes.

B. Divertissement: The plastic case

Following the view that it does not matter how λ is taken from its initial value to its final value, we have performed simulations with greater imposed penetrations where the mechanical response changes drastically. Rather than elastic reversible deformations, our indentation process with $\lambda_{max} > 4.5$ Å leads to (irreversible) crystal plasticity, i.e., deformations of the crystal that persist in time due to the formation of crystalline defects underneath the indenter.[37] Then, besides the difficulties encountered to verify the JE in the purely elastic case, a new condition emerges that is complex to describe using equilibrium statistical mechanics. Irreversibility, thus, emerges from the reversible dynamics of a rather small Hamiltonian system when λ_{max} is increased.

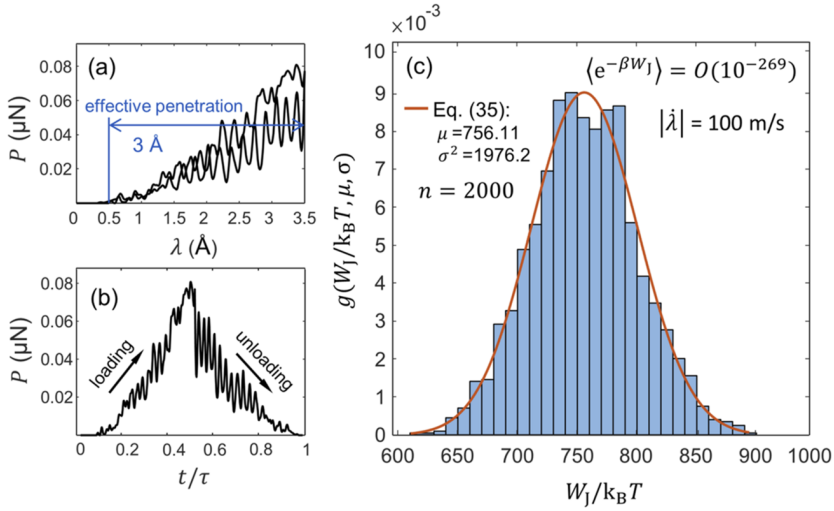

FIG. 5. Elastic case performed at $|\dot{\lambda}| = 100$ m/s ($\tau = 7$ ps). (a) and (b) Load evolution in a single realization. (c) The PDF of the W_J data from 2000 realizations.

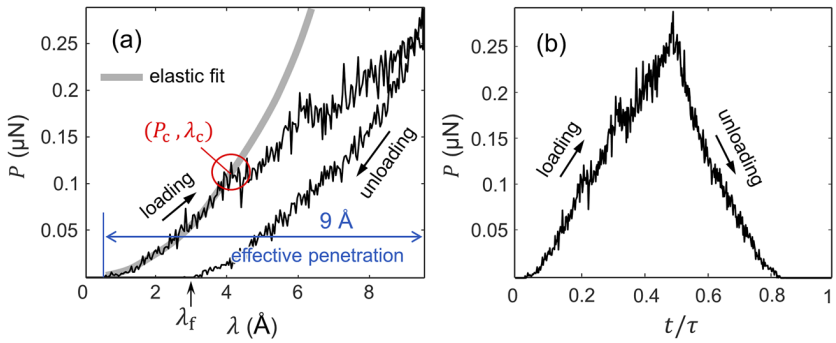

FIG. 6. Single realization of the plastic case at $|\dot{\lambda}| = 10$ m/s ($\tau = 190$ ps), where $\lambda_{max} = 9.5$ Å. (a) and (b) $P - \lambda$ and $P - t/\tau$ curves, respectively. The gray line in (a) represents the elastic fit given by the Hertzian contact theory, where $P \sim (\lambda - \Delta)^{3/2}$. The process is characterized by irreversibility due to the plasticity evidenced by the utterly mismatched load and unload paths. Note in (a) that departure from the elastic behavior starts at a critical load $P_c \approx 0.11$ μN at $\lambda_c \approx 4$ Å.

The plastic indentation case studied here is a load/unload process with $\lambda_{max} = 0.3R + \Delta = 9.5$ Å; see Fig. 1(c). In the simulations, the elastic behavior is clearly violated at values of $\lambda \approx \lambda_{max}/2$ during the loading stage; cf. Fig. 6. Therefore, the imposed λ_{max} is well within the λ range in which plastic features can be observed in the $P - \lambda$ curves. The load evolutions obtained in single-realization runs are given in Fig. 6.

The resulting $P - \lambda$ curves are characterized by an early elastic response followed by a load drop at the inception of plasticity (Fig. 6).[38] With increasing λ, further load drops result from the activation of additional plastic processes in the crystal, where the $P - \lambda$ evolution fundamentally diverges from the elastic fit. During unloading, the force vanishes with λ values greater than Δ; e.g., see in Fig. 6(a), where $\lambda_f \approx 3$ Å. In this regard, steep unloading curves are a fundamental manifestation of the generation of a plastic imprint induced during the indentation process, which remains in the particle system upon the removal of the indenter tip from the surface. In addition, this feature leads to an absolute value of the work done during loading that is greater than that done during unloading, thus resulting in relatively large W_J; see Fig. 7. For further details of such indentation responses in metals using nanometer-sized indenter tips, the reader is referred to Refs. 34 and 37.

When the W_J data are fitted, the resulting PDF reveals a clear tendency to develop some skewness, while the average and the variance take values of $\mu \approx 0.576$ nano-erg [$\approx 13,960$ in dimensionless $W_J/(k_B T)$ units] and $\sigma^2 \approx 4.8$ nano-erg^2. Figure 8 shows the left-skewed W_J distribution of the plastic process.

In addition, note that in the elastic (reversible) case, we obtained larger values for $\langle e^{-\beta W_J} \rangle_\alpha$ that range from ≈3 to ≈37 (with $n = 1000$), which are still computable in terms of Eq. (19). On the contrary, in the case of the plastic (irreversible) indentations with $n = 2000$, we have large positive values for W_J so $\langle e^{-\beta W_J} \rangle_\alpha$ converges to 0 and $\Delta F^*_{\alpha \to \omega}$ in Eq. (19) cannot be handled numerically. For instance, we find that the quantity $-\beta \langle W_J \rangle_\alpha$ is of the order of $O(10^{22})$ in the plastic process with $n = 2000$; see Fig. 8. Actually, the numerical analysis of the right-hand side of Eq. (19), which should be 1, drastically misses this target value in all indentation tests.

V. DISCUSSION

Our MD investigation of indentation on a Ta crystal composed of $O(10^4)$ atoms completely fails to reproduce the correct value of the left-hand side of Eq. (19) although

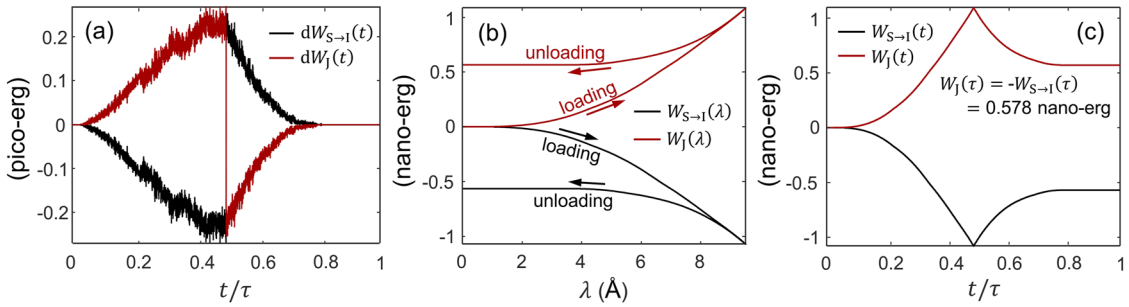

FIG. 7. Evolution of the works W_J, $W_{S\to I}$, and $W_{I\to S}$, defined by Eqs. (33) and (34) and measured in erg, for single realizations of the indentation process at $|\dot{\lambda}| = 10$ m/s ($\tau = 190$ ps). (a) illustrates the elementary works $dW_{S\to I}$ and dW_J done over an infinitesimal time of $dt = 0.5$ ps. (b) and (c) give the evolution of $W_{S\to I}$ and W_J as functions of λ and t/τ, respectively.

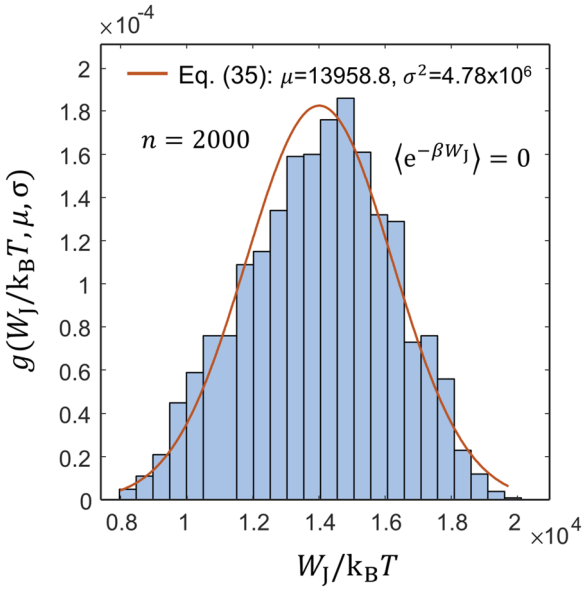

FIG. 8. PDF of the W_J data from 2000 realizations of the plastic case with $|\dot{\lambda}|$ = 10 m/s. The curve g represents the Gaussian approximation of the normalized histogram of the W_J/k_BT data.

1. the dynamics of S + E and of the indenter are cast in a Hamiltonian formalism,
2. only the energy of S is affected by the moving potential representing the indenter, and
3. the initial conditions on which we estimate the expected values are sampled from a canonical distribution.

These are the conditions required in the formal derivation of the JE. In addition, our system is not large, and in the case of the slow elastic indentations, we avoid any evident onset of irreversibility. Since our numerical analysis can compute W_J, the difficulty of verifying the JE must then be of a subtler nature than what the formalism readily reveals.

Our first observation is that the problem is not merely statistical. The sampling problem exists and has been evidenced in various works, beginning with the original paper.[9] In Ref. 19, it has also been shown that even in the simple case of adiabatic expansion of an ideal gas, the number of repetitions of the experiment required to verify the JE grows exponentially with the size of the system. Consequently, the JE rapidly turns unverifiable, for statistical reasons, even when it correctly represents a property of the system. To check whether this or more fundamental effects prevented the verification of the JE, we have performed two tests suggested by one of the referees. For the elastic indentation cases with $|\dot{\lambda}|$ = 1 and 10 m/s, we have first computed the following quantity:

$$V = \frac{\langle W_J \rangle_\alpha - \Delta F_S^*}{k_B T}, \tag{36}$$

where $\Delta F_S^* = 0$ corresponds to our cases. It is noted that large values of this quantity indicate that the verification of the JE may be difficult, thus requiring larger statistics.[17] We have obtained $V \approx 6$ and $V \approx 14$ for $|\dot{\lambda}|$ = 1 and 10 m/s, respectively. This first test suggests that the JE should be verifiable for $|\dot{\lambda}|$ = 1 m/s and that the outcome should be closer to the JE prediction than for $|\dot{\lambda}|$ = 10 m/s. However, we have not been able to verify the JE in either case. Moreover, the estimation of the free-energy difference for $|\dot{\lambda}|$ = 1 m/s is worse than that for $|\dot{\lambda}|$ = 10 m/s. This is illustrated in Fig. 9 in connection with the second test, where we plot the estimated value of the free-energy difference,

$$\Delta F_S^{*\mathrm{est}}(n) = -\frac{1}{\beta} \ln\left(\frac{1}{n} \sum_{l=1}^{n} e^{-\beta W_{J,l}} \right), \tag{37}$$

as a function of the ensemble size n. For $|\dot{\lambda}|$ = 1 m/s, we find that $\Delta F_S^{*\mathrm{est}}$ gradually settles at ≈ − 0.16 pico-erg (and not at 0) as n grows up to n = 1000. For $|\dot{\lambda}|$ = 10 m/s, $\Delta F_S^{*\mathrm{est}}$ takes about −0.06 pico-erg, which is thus closer to 0.

While in some cases improved statistics or statistical techniques may solve the problem, in other cases, the predictions may be simply incorrect. The latter seems to be the case regarding our numerical simulations of the plastic deformations, which the JE cannot describe. In this context, it can be useful to consider Refs. 22 and 39, which refer to systems that, after a perturbation, by definition cannot restore their original state.

It is, however, even more interesting to note that the JE may fail even in the absence of the above extreme (irreversible) situations. In the elastic cases, certain fluctuations of W_J produced by an external intervention can never be observed despite being apparently allowed by certain initial conditions. For instance, these fluctuations include deformations of the crystal working against the action of the indenter, which would translate into large negative values of W_J. Although weighted with exceedingly low probabilities, these negative W_J values could give a substantial contribution as they are multiplied by

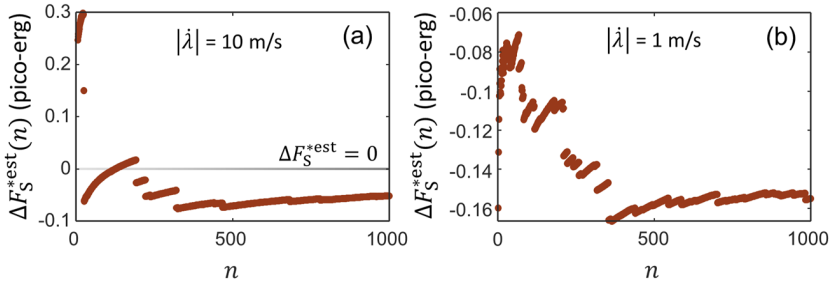

FIG. 9. Estimated values of the free-energy difference associated with the elastic indentation processes. The quantity $\Delta F_S^{*\mathrm{est}}$ defined by Eq. (37) is plotted as a function of the ensemble size n, using the data from the MD indentations with $|\dot{\lambda}|$ = 10 m/s (a) and 1 m/s (b). The discontinuities in the values of $\Delta F_S^{*\mathrm{est}}(n)$ gradually decrease with growing n, as expected.

$-\beta$ and exponentiated. However, a complete sampling of the canonical ensemble would be needed, and that results unworkable. Even when possible, in principle, it requires an infinite amount of time. The fact is that the dynamics improperly explores the final canonical equilibrium at temperature T and $\lambda = \omega$. The trajectories sampled as typical from the initial equilibrium ensemble are unsuitable to correctly span the range of typical values of the observables of interest in the final equilibrium state.

These observations concern both elastic and plastic deformations occurring in the crystal. In the latter, energy is lost in the unloading stage of the hysteresis cycle. In particular, plastic deformations manifest the emergence of irreversible phenomena in the system, within the reversible, fully conservative, classical mechanical scheme of the Jarzynski theory. While this could, in principle, be quantified and taken into account to restore the validity of the JE, the limited exploration of the ensemble and the finite size effects are exacerbated. Then, the fact that the system does not recover its initial state directly implies, even in principle, not just in practice, a violation of the JE: a violation that is not eased by any collection of statistics, be it finite or infinitely large.

The notion that irreversible phenomena may violate the JE is known, although the impact of irreversibility is not always disruptive; see, e.g., Refs. 40–42. For instance, Ref. 7 notes that the JE fails in chaotic dissipative systems,[43] in active matter,[44] and also for the strongly irreversible systems of Refs. 22 and 39. Such scenarios, however, lie outside the framework of the JE. The question is whether anything similar may happen within the JE framework. We show that it does. In our indentation case irreversibility is an emergent phenomenon of (reversible) Hamiltonian dynamics related not just to the size of the system[5] but also to the process being performed. It is perhaps even more interesting that there is no need to reach such degrees of irreversibility. All of our indentation processes violate the JE, including the fully reversible elastic indentations.

To sum up, our main arguments highlight and clarify the following:

1. It is impossible to verify the JE in indentation processes such as ours, although they concern small systems fully complying with the requirements under which the JE is formally derived.
2. The results depend on the work process because it is impossible to sample the regions of phase space required by the theory.
3. The JE does not compute, in general, the free-energy difference of the system; cf. Eq. (9). It computes the free-energy difference of the system and environment together; cf. Eq. (18).
4. Although in our investigation, the quantity W_J can be identified with a mechanical or thermodynamic work, this consideration is not universal.
5. Emergent, process-dependent plastic deformations of Hamiltonian systems with a fixed number of particles complying with the JE framework violate the JE because the undeformed state is not restored.

ACKNOWLEDGMENTS

L.R. acknowledges partial support from Ministero dell'Università e della Ricerca (Italy), grant Dipartimenti di Eccellenza 2018–2022 (Grant No. E11G18000350001). The work of J.V. was supported by Ministerstvo Školství, Mládeže a Tělovýchovy (Czech Republic) through the European Structural and Investment Fund project "Center of Excellence for Nonlinear Dynamic Behavior of Advanced Materials in Engineering (CeNDYNMAT)" (Grant No. CZ.02.1.01/0.0/0.0/15_003/0000493), with institutional support RVO:61388998. J.A. acknowledges financial support by Ministerio de Ciencia e Innovación (Grant No. PID2019-106744GB-I00 to the UPC).

AUTHOR DECLARATIONS

Conflict of Interest

The authors have no conflicts of interest to disclose.

Author Contributions

All authors contributed equally to this work.

DATA AVAILABILITY

The data that support the findings of this study are available from the corresponding author upon reasonable request.

REFERENCES

[1] E. Fermi, *Thermodynamics* (Dover Publications, New York, 1956).
[2] H. B. Callen. *Thermodynamics and an Introduction to Thermostatistics* (John Wiley & Sons, New York, 1985).
[3] H. Spohn, *Large Scale Dynamics of Interacting Particles* (Springer-Verlag, 1991).
[4] D. Jou, G. Lebon, and J. Casas-V'azquez, *Extended Irreversible Thermodynamics* (Springer-Verlag, 2010).
[5] S. Chibbaro, L. Rondoni, and A. Vulpiani, *Reductionism, Emergence and Levels of Reality: The Importance of Being Borderline* (Springer-Verlag, 2014).
[6] L. Rondoni, "Introduction to nonequilibrium statistical physics and its foundations," in *Frontiers and Progress of Current Soft Matter Research*, edited by X.-Y. Liu (Springer, Singapore, 2021), pp. 1–82.
[7] S. Ciliberto, "Experiments in stochastic thermodynamics: Short history and perspectives," Phys. Rev. X **7**, 021051 (2017).
[8] From this point of view, protein stretching experiments are noteworthy, since they are dissipative and look rather different from low dimensional Langevin processes.[29]
[9] C. Jarzynski, "Nonequilibrium equality for free energy differences," Phys. Rev. Lett. **78**, 2690–2693 (1997).
[10] C. Jarzynski, "Nonequilibrium work theorem for a system strongly coupled to a thermal environment," J. Stat. Mech.: Theory Exp. **2004**, P09005.
[11] T. Schmiedl and U. Seifert, "Optimal finite-time processes in stochastic thermodynamics," Phys. Rev. Lett. **98**, 108301 (2007).
[12] A. Gomez-Marin, T. Schmiedl, and U. Seifert, "Optimal protocols for minimal work processes in underdamped stochastic thermodynamics," J. Chem. Phys. **129**, 024114 (2008).
[13] E. Aurell, C. Mejía-Monasterio, and P. Muratore-Ginanneschi, "Optimal protocols and optimal transport in stochastic thermodynamics," Phys. Rev. Lett. **106**, 250601 (2011).
[14] E. Aurell, C. Mejía-Monasterio, and P. Muratore-Ginanneschi, "Boundary layers in stochastic thermodynamics," Phys. Rev. E **85**, 020103 (2012).
[15] P. Muratore-Ginanneschi, "On the use of stochastic differential geometry for non-equilibrium thermodynamics modeling and control," J. Phys. A: Math. Theor. **46**, 275002 (2013).
[16] S. J. Davie *et al.*, "Applicability of optimal protocols and the Jarzynski equality," Phys. Scr. **89**, 048002 (2014).
[17] T. R. Gingrich *et al.*, "Near-optimal protocols in complex nonequilibrium transformations," Proc. Natl. Acad. Sci. **113**, 10263–10268 (2016).

[18]G. Ciccotti and L. Rondoni, "Jarzynski on work and free energy relations: The case of variable volume," AIChE J. **67**, e17082 (2021).
[19]R. C. Lua and A. Y. Grosberg, "Practical applicability of the Jarzynski relation in statistical mechanics: A pedagogical example," J. Phys. Chem. B **109**, 6805–6811 (2005).
[20]Ref. 9 states: "*Since such values of the work represent statistically very rare events, it would require an unreasonably large number of measurements of W to determine with accuracy*." "*This condition pretty much rules out macroscopic systems of interest*." Here, $\beta = 1/k_B T$ and W is the quantity identified as work in Ref. 9.
[21]C. Jarzynski, "Rare events and the convergence of exponentially averaged work values," Phys. Rev. E **73**, 046105 (2006).
[22]Y. Murashita, "Absolute irreversibility in information thermodynamic," M.A. thesis, University of Tokyo, 2015.
[23]J. W. Gibbs, *Elementary Principles in Statistical Mechanics* (Scribner's Sons, 1902).
[24]C. Jarzynski, "Stochastic and macroscopic thermodynamics of strongly coupled systems," Phys. Rev. X **7**(1), 011008 (2017).
[25]J. G. Kirkwood, "Statistical Mechanics of fluid mixtures," J. Chem. Phys. **3**, 300–313 (1935).
[26]Note that the equilibria at which Eq. (11) holds are not realized during the JE process, except at time $t = 0$.
[27]The fact that $U^*(\tau, \omega)$ depends on τ is not *per se* a problem; it is a τ-dependent f_α-equilibrium quantity at fixed ω.
[28]This case is analogous to those investigated in Refs. 22 and 39, in which the initial state cannot be restored after a perturbation. In that highly idealized case, explicit calculations are possible and show that the JE must be modified. Then, the verification of the JE is not merely statistically difficult, as this equality is fundamentally inaccurate.
[29]A. M. Monge, M. Manosas, and F. Ritort, "Experimental test of ensemble inequivalence and the fluctuation theorem in the force ensemble in DNA pulling experiments," Phys. Rev. E **98**, 032146 (2018).
[30]S. Plimpton, "Fast parallel algorithms for short-rangemolecular dynamics," J. Comput. Phys. **117**, 1–19 (1995).
[31]C. L. Kelchner, S. J. Plimpton, and J. C. Hamilton, "Dislocation nucleation and defect structure during surface indentation," Phys. Rev. B **58**, 11085–11088 (1998).
[32]G. Ziegenhain, A. Hartmaier, and H. M. Urbassek, "Pair vs many-body potentials: Influence on elastic and plastic behavior in nanoindentation of fcc metals," J. Mech. Phys. Solids **57**, 1514–1526 (2009).
[33]T. P. Remington *et al.*, "Plastic deformation in nanoindentation of tantalum: A new mechanism for prismatic loop formation," Acta Mater. **78**, 378–393 (2014).
[34]J. Varillas *et al.*, "Unraveling deformation mechanisms around FCC and BCC nanocontacts through slip trace and pileup topography analyses," Acta Mater. **125**, 431–441 (2017).
[35]R. Ravelo *et al.*, "Shock-induced plasticity in tantalum single crystals: Interatomic potentials and large-scale molecular-dynamics simulations," Phys. Rev. B **88**, 134101 (2013).
[36]K. L. Johnson, *Contact Mechanics* (Cambridge University Press, 1985).
[37]J. Varillas *et al.*, "Understanding imprint formation, plastic instabilities and hardness evolutions in FCC, BCC and HCP metal surfaces," Acta Mater. **217**, 117122 (2021).
[38]Similar drops are observed in DNA pulling experiments Ref. 29.
[39]Y. Murashita, K. Funo, and M. Ueda, "Nonequilibrium equalities in absolutely irreversible processes," Phys. Rev. E **90**, 042110 (2014).
[40]L. Rondoni and E. Segre, "Fluctuations in two-dimensional reversibly damped turbulence," Nonlinearity **12**, 1471 (1999).
[41]G. Gallavotti, L. Rondoni, and E. Segre, "Lyapunov spectra and nonequilibrium ensembles equivalence in 2D fluid mechanics," Physica D **187**, 338 (2004).
[42]M. Colangeli and L. Rondoni, "Equilibrium, fluctuation relations and transport for irreversible deterministic dynamics," Physica D **241**, 681 (2012).
[43]S. Ciliberto, R. Gomez-Solano, and A. Petrosyan, "Fluctuations, linear response, and currents in out-of-equilibrium systems," Annu. Rev. Condens. Matter Phys. **4**, 235–261 (2013).
[44]C. Bechinger *et al.*, "Active particles in complex and crowded environments," Rev. Mod. Phys. **88**, 045006 (2016).